



Revised error propagation of $^{40}\text{Ar}/^{39}\text{Ar}$ data, including covariances

Pieter Vermeesch

Department of Earth Sciences, University College London, United Kingdom

Received 14 May 2015; accepted in revised form 14 September 2015; available online 25 September 2015

Abstract

The main advantage of the $^{40}\text{Ar}/^{39}\text{Ar}$ method over conventional K–Ar dating is that it does not depend on any absolute abundance or concentration measurements, but only uses the relative ratios between five isotopes of the same element – argon – which can be measured with great precision on a noble gas mass spectrometer. The relative abundances of the argon isotopes are subject to a constant sum constraint, which imposes a covariant structure on the data: the relative amount of any of the five isotopes can always be obtained from that of the other four. Thus, the $^{40}\text{Ar}/^{39}\text{Ar}$ method is a classic example of a ‘compositional data problem’. In addition to the constant sum constraint, covariances are introduced by a host of other processes, including data acquisition, blank correction, detector calibration, mass fractionation, decay correction, interference correction, atmospheric argon correction, interpolation of the irradiation parameter, and age calculation. The myriad of correlated errors arising during the data reduction are best handled by casting the $^{40}\text{Ar}/^{39}\text{Ar}$ data reduction protocol in a matrix form. The completely revised workflow presented in this paper is implemented in a new software platform, *Ar–Ar_Redux*, which takes raw mass spectrometer data as input and generates accurate $^{40}\text{Ar}/^{39}\text{Ar}$ ages and their (co-)variances as output. *Ar–Ar_Redux* accounts for all sources of analytical uncertainty, including those associated with decay constants and the air ratio. Knowing the covariance matrix of the ages removes the need to consider ‘internal’ and ‘external’ uncertainties separately when calculating (weighted) mean ages. *Ar–Ar_Redux* is built on the same principles as its sibling program in the U–Pb community (*U–Pb_Redux*), thus improving the intercomparability of the two methods with tangible benefits to the accuracy of the geologic time scale. The program can be downloaded free of charge from <http://redux.london-geochron.com>.

© 2015 Elsevier Ltd. All rights reserved.

1. INTRODUCTION

Let z be a function f of two variables x and y :

$$z = f(x, y) \quad (1)$$

then standard error propagation of z by first order Taylor expansion yields:

$$\sigma_z^2 = \left(\frac{\partial f}{\partial x}\right)^2 \sigma_x^2 + \left(\frac{\partial f}{\partial y}\right)^2 \sigma_y^2 + 2 \frac{\partial f}{\partial x} \frac{\partial f}{\partial y} \text{cov}(x, y) \quad (2)$$

where $\text{cov}(x, y)$ is the ‘covariance of x and y ’. Current practice in $^{40}\text{Ar}/^{39}\text{Ar}$ geochronology generally assumes that the third term of Eq. (2) can be safely neglected. For example, consider the $^{40}\text{Ar}/^{39}\text{Ar}$ age equation:

$$T = \ln(1 + JR) / \lambda_{40} \quad (3)$$

with λ_{40} the decay constant of ^{40}K , J the neutron irradiation parameter (see Section 11) and R the $^{40}\text{Ar}^*/^{39}\text{Ar}_K$ -ratio (where $^{40}\text{Ar}^*$ is the radiogenic argon component and $^{39}\text{Ar}_K$ is derived from neutron reactions on ^{39}K). Then the age uncertainty is currently calculated as Berger and

E-mail address: p.vermeesch@ucl.ac.uk

York (1970), McDougall and Harrison (1999) and Koppers (2002):

$$\sigma_T^2 = \frac{J^2 \sigma_R^2 + R^2 \sigma_J^2}{\lambda_{40}^2 (1 + RJ)} \quad (4)$$

which assumes that $cov(R, J) = 0$. This assumption cannot be correct because both R and J are calculated using the same mass fractionation corrections, detector calibrations, interference corrections and radioactive decay corrections. The analytical uncertainty associated with each of these factors results in correlated errors between R and J . Ignoring these error correlations affects both the precision and accuracy of the resulting $^{40}\text{Ar}/^{39}\text{Ar}$ ages.

The problem of correlated errors is not limited to R and J alone. It crops up literally everywhere in the $^{40}\text{Ar}/^{39}\text{Ar}$ method. In fact, a covariant structure is deeply engrained into the very DNA of the method, which is based on five isotopes (36–40) of a single element (Ar). This paper will show that, because the $^{40}\text{Ar}/^{39}\text{Ar}$ method is based on ratios rather than absolute abundances, it is subject to the peculiar mathematics of ‘compositional data’ (Section 2). Correlated errors are created during mass spectrometry, when the ion detector signals are extrapolated to ‘time zero’ and blank corrections are made (Sections 3 and 4). They occur as a result of mass fractionation corrections and detector inter-calibrations (Section 5). They arise when accounting for the effect of radioactive decay on ^{39}Ar (from K), ^{36}Ar (from Cl) and ^{37}Ar (from Ca) (Section 7), or whenever an interference correction is made (Section 8). Error correlations occur when calculating J -factors (Section 11) and, as we have already seen at the beginning of this section, when applying the J -factor to solve the age equation (Section 12). Error correlations must also be taken into account when calculating the weighted mean of several $^{40}\text{Ar}/^{39}\text{Ar}$ age analyses (Section 13). Finally, the methods presented in this paper provide a simple and elegant way to account for the systematic biases that occur as a result of the uncertainty in the ^{40}K decay constant and the atmospheric $^{40}\text{Ar}/^{36}\text{Ar}$ ratio (Section 12).

Thus, the existence of correlated errors affects every aspect of the $^{40}\text{Ar}/^{39}\text{Ar}$ method. The paper at hand presents an analytical solution to this problem as an alternative to the numerical approximations proposed elsewhere (Scaillet, 2000). A new computer code called Ar-Ar_Redux was developed with the aim to facilitate the adoption of the rigorous data reduction and error propagation methods presented herein (Section 14).

2. $^{40}\text{Ar}/^{39}\text{Ar}$ AS A COMPOSITIONAL DATA PROBLEM

As mentioned in Section 1, the $^{40}\text{Ar}/^{39}\text{Ar}$ -age calculation is based on the $^{40}\text{Ar}^*/^{39}\text{Ar}_K$ -ratio (R , see Eq. (3)), which can be calculated as follows:

$$R = \frac{1 - a + b + c}{d - e} - f \quad (5)$$

with

$$a = \left[\frac{^{40}\text{Ar}}{^{36}\text{Ar}} \right]_a \left[\frac{^{36}\text{Ar}}{^{40}\text{Ar}} \right]_m \quad (6)$$

$$b = \left[\frac{^{40}\text{Ar}}{^{36}\text{Ar}} \right]_a \left[\frac{^{36}\text{Ar}}{^{37}\text{Ar}} \right]_{ca} \left[\frac{^{37}\text{Ar}}{^{40}\text{Ar}} \right]_m \quad (7)$$

$$c = \left[\frac{^{40}\text{Ar}}{^{36}\text{Ar}} \right]_a \left[\frac{^{36}\text{Ar}}{^{38}\text{Ar}} \right]_{cl} \left[\frac{^{38}\text{Ar}}{^{40}\text{Ar}} \right]_m \quad (8)$$

$$d = \left[\frac{^{39}\text{Ar}}{^{40}\text{Ar}} \right]_m \quad (9)$$

$$e = \left[\frac{^{39}\text{Ar}}{^{37}\text{Ar}} \right]_{ca} \left[\frac{^{37}\text{Ar}}{^{40}\text{Ar}} \right]_m \quad (10)$$

$$f = \left[\frac{^{40}\text{Ar}}{^{39}\text{Ar}} \right]_k \quad (11)$$

in which ‘ a ’ stands for ‘air’, ‘ ca ’ for ‘Ca-salt’, ‘ k ’ for ‘K-glass’, and ‘ cl ’ for ‘Cl decay products’. The subscript ‘ m ’ stands for either ‘sample’ or ‘fluence monitor’. The meaning of this equation and the significance of the subscripts will be elaborated in later sections of this paper. The important point which needs to be made here is that Eqs. (6)–(11) only contain ratios, and do not depend on the absolute abundances of the different argon isotopes. In statistical terms, $^{40}\text{Ar}/^{39}\text{Ar}$ -measurements are said to be ‘compositional data’ and are subject to the peculiar mathematics of the compositional dataspace or ‘simplex’ (Aitchison, 1986). To illustrate the profound implications of this point, consider the simple situation of a K -bearing sample containing neither Ca nor Cl. In this case, terms b , c and e in Eq. (5) disappear, which leaves us with a simple three component system comprised of ^{36}Ar , ^{39}Ar and ^{40}Ar . Because we are only interested in the relative abundances of these three isotopes, they can be normalised to unity and plotted on a ternary diagram (Fig. 1). It is well known that common summary statistics such as the arithmetic mean and standard deviation are unreliable in this data space. This is because the ternary diagram occupies a narrowly restricted subspace of the realm of real numbers. These restrictions cause problems because standard data reduction methods commonly assume that the data follow a Normal distribution, which requires support from $-\infty$ to $+\infty$. The solution to this conundrum is to transform the data from the simplex to a Euclidean ‘logratio space’, in which standard Normal theory can be safely used (Aitchison, 1986; Vermeesch, 2010).

In addition to opening compositional data to standard statistical analysis, the logratio transformation also simplifies the algebra of $^{40}\text{Ar}/^{39}\text{Ar}$ data reduction. This is because many of the calculations required for processing $^{40}\text{Ar}/^{39}\text{Ar}$ -data involve multiplication and exponentiation, which reduce to simple addition and multiplication after taking logs. The next sections of this paper will show how the raw mass spectrometric data can be cast into a logratio covariance structure for further processing, for both multi-collector (Section 3) and single collector (Section 4) instruments.

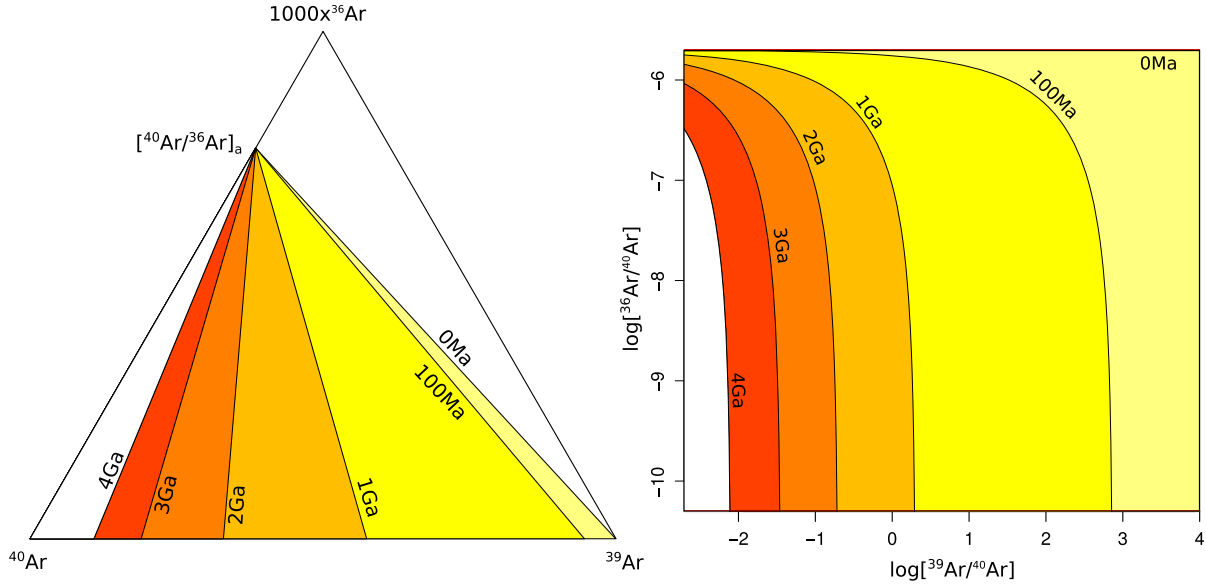


Fig. 1. $^{40}\text{Ar}/^{39}\text{Ar}$ -data are compositional data, in which only the ratios between components matter, and not their absolute abundances. This is reflected in the fact that ^{40}Ar – ^{39}Ar – ^{36}Ar data can be renormalised to unity and plotted on a ternary diagram (left). There is a one-to-one mapping between this so-called ‘simplex’ and Euclidean logratio space (right).

3. MULTI-COLLECTOR DATA

To illustrate the calculations in the remainder of this paper, consider the following sequence of analyses: b_1 (first blank), u_1 (first sample), s_1 (first age standard), u_2 (second sample), b_2 (second blank), s_2 (second standard), s_3 (third standard) and b_3 (third blank). In a multicollector mass spectrometer, each of the five argon isotopes appearing in Eq. (5) are monitored simultaneously through time (t) and can be cast into an $[n \times 5]$ matrix format, with n the number of integrations (i.e. $t = \{t_1, t_2, \dots, t_n\}$):

$$M(x, t) = \begin{bmatrix} {}^{36}\text{Ar}(x, t_1) & {}^{37}\text{Ar}(x, t_1) & {}^{38}\text{Ar}(x, t_1) & {}^{39}\text{Ar}(x, t_1) & {}^{40}\text{Ar}(x, t_1) \\ {}^{36}\text{Ar}(x, t_2) & {}^{37}\text{Ar}(x, t_2) & {}^{38}\text{Ar}(x, t_2) & {}^{39}\text{Ar}(x, t_2) & {}^{40}\text{Ar}(x, t_2) \\ \vdots & \vdots & \vdots & \vdots & \vdots \\ {}^{36}\text{Ar}(x, t_n) & {}^{37}\text{Ar}(x, t_n) & {}^{38}\text{Ar}(x, t_n) & {}^{39}\text{Ar}(x, t_n) & {}^{40}\text{Ar}(x, t_n) \end{bmatrix} \quad (12)$$

where ‘ x ’ stands for ‘blank’, ‘sample’ or ‘standard’. The same formulation can be used for the interference monitors (particularly Ca) but further discussion of these will be deferred to Section 8 and Appendix A. Because the measurements are done simultaneously on all five detectors, any random variation in, say, the filament voltage or trap current will simultaneously affect all signals, resulting in correlated residuals. The blank correction is made by subtracting the time-resolved signal of the nearest blank measurement (b) from that of the analysis (x), resulting in a new matrix $B(x, b, t)$:

$$B(x, b, t) = \begin{bmatrix} {}^{36}\text{Ar}^b(x, t_1) & {}^{37}\text{Ar}^b(x, t_1) & {}^{38}\text{Ar}^b(x, t_1) & {}^{39}\text{Ar}^b(x, t_1) & {}^{40}\text{Ar}^b(x, t_1) \\ {}^{36}\text{Ar}^b(x, t_2) & {}^{37}\text{Ar}^b(x, t_2) & {}^{38}\text{Ar}^b(x, t_2) & {}^{39}\text{Ar}^b(x, t_2) & {}^{40}\text{Ar}^b(x, t_2) \\ \vdots & \vdots & \vdots & \vdots & \vdots \\ {}^{36}\text{Ar}^b(x, t_n) & {}^{37}\text{Ar}^b(x, t_n) & {}^{38}\text{Ar}^b(x, t_n) & {}^{39}\text{Ar}^b(x, t_n) & {}^{40}\text{Ar}^b(x, t_n) \end{bmatrix} \quad (13)$$

with

$${}^i\text{Ar}^b(x, t_j) = {}^i\text{Ar}(x, t_j) - {}^i\text{Ar}(b, t_j) \quad (14)$$

for $i = \{36, 37, 38, 39, 40\}$ and $j = \{1, \dots, n\}$. Our goal is to extract 4-element vectors of logratios from these $[n \times 5]$ matrices of blank corrected mass spectrometer signals, taking into account any correlated errors. The easiest but by no means only way to achieve this is by forming the logratios prior to regression, yielding an $[n \times 4]$ matrix for each analysis:

$$L(x, b, t) = \begin{bmatrix} l \left[\frac{{}^{36}\text{Ar}^b(x, t_1)}{{}^{40}\text{Ar}^b(x, t_1)} \right] & l \left[\frac{{}^{37}\text{Ar}^b(x, t_1)}{{}^{40}\text{Ar}^b(x, t_1)} \right] & l \left[\frac{{}^{38}\text{Ar}^b(x, t_1)}{{}^{40}\text{Ar}^b(x, t_1)} \right] & l \left[\frac{{}^{39}\text{Ar}^b(x, t_1)}{{}^{40}\text{Ar}^b(x, t_1)} \right] \\ l \left[\frac{{}^{36}\text{Ar}^b(x, t_2)}{{}^{40}\text{Ar}^b(x, t_2)} \right] & l \left[\frac{{}^{37}\text{Ar}^b(x, t_2)}{{}^{40}\text{Ar}^b(x, t_2)} \right] & l \left[\frac{{}^{38}\text{Ar}^b(x, t_2)}{{}^{40}\text{Ar}^b(x, t_2)} \right] & l \left[\frac{{}^{39}\text{Ar}^b(x, t_2)}{{}^{40}\text{Ar}^b(x, t_2)} \right] \\ \vdots & \vdots & \vdots & \vdots \\ l \left[\frac{{}^{36}\text{Ar}^b(x, t_n)}{{}^{40}\text{Ar}^b(x, t_n)} \right] & l \left[\frac{{}^{37}\text{Ar}^b(x, t_n)}{{}^{40}\text{Ar}^b(x, t_n)} \right] & l \left[\frac{{}^{38}\text{Ar}^b(x, t_n)}{{}^{40}\text{Ar}^b(x, t_n)} \right] & l \left[\frac{{}^{39}\text{Ar}^b(x, t_n)}{{}^{40}\text{Ar}^b(x, t_n)} \right] \end{bmatrix} \quad (15)$$

where ‘ l ’ stands for ‘natural log’ and ${}^{40}\text{Ar}$ is used as a common denominator for all the ratios denoted by ‘ m ’ in Eq. (5). We thus obtain five time-resolved logratio matrices, one for each run in the analysis sequence. These five matrices can be assembled into one $[n \times 20]$ matrix, which is naturally partitioned into three groups by the blanks.

$$G(t) = [L(u_1, b_1, t) | L(s_1, b_1, t) | L(u_2, b_2, t) | L(s_2, b_2, t) | L(s_3, b_3, t)] \\ = [g_1 | g_2 | g_3] \quad (16)$$

where the first group (g_1) consists of sample u_1 and standard s_1 , which share blank b_1 ; the second group (g_2) consists of sample u_2 and standard s_2 , which share blank b_2 ; and the third group consists of standard s_3 , which is the only analysis using blank b_3 . It is reasonable to expect the blank-corrected logratio signals to be correlated within each group, but uncorrelated between groups. We therefore

extrapolate the logratio signals to $t = 0$ ('time zero') in blocks, and concatenate the resulting logratio intercepts into a single 20-element vector:

$$X = [X(g_1) X(g_2) X(g_3)] \quad (17)$$

with $X(g_i)$ the vector of logratio intercepts of the i th group, obtained by joint (non)linear regression. The $[20 \times 20]$ covariance matrix of X is given by:

$$\Sigma_X = \begin{bmatrix} \Sigma_{g_1} & 0_{8,8} & 0_{8,4} \\ 0_{8,8} & \Sigma_{g_2} & 0_{8,4} \\ 0_{4,8} & 0_{4,8} & \Sigma_{g_3} \end{bmatrix} \quad (18)$$

where Σ_{g_i} is the covariance matrix of the i th group's intercepts and $0_{i,j}$ denotes a zero matrix of size $[i \times j]$. One well known problem with the logratio transformation is the handling of zero or negative values. In the context of argon mass spectrometry, this occurs in one of two situations: (a) ^{36}Ar (and ^{38}Ar) in the atmospheric correction of extremely clean samples and (b) ^{37}Ar in the Ca-interference correction of 'expired' samples. The zero value problem can be avoided by performing generalised linear regression of the ratios (using a logarithmic link function to ensure positive intercepts, [Nelder and Wedderburn, 1972](#)), or to cast the regression problem into a more sophisticated maximum likelihood form ([Wood, 2015](#)). A comprehensive discussion of these alternative methods falls outside the scope of the present paper and will be deferred to a future publication.

4. 'PEAK-HOPPING' DATA

In single collector mass spectrometers, the various argon isotopes cannot be monitored simultaneously, but must be measured separately. This is achieved by separately scanning ('hopping') over the mass range of the argon isotopes by varying the field strength of the mass analyser. Thus, each mass has its own time scale t^i , for $i = 36, 37, 38, 39$ and 40, resulting in a set of five time resolved data vectors $M(x, i, t^i)$ for each run x :

$$M(x, i, t^i) = \begin{bmatrix} {}^i\text{Ar}(x, t_1^i) \\ {}^i\text{Ar}(x, t_2^i) \\ \vdots \\ {}^i\text{Ar}(x, t_n^i) \end{bmatrix} \quad (19)$$

Because the five isotope signals are measured at different times, we can safely assume their residual noise to be uncorrelated. Again, blank correction is done in time-resolved mode, but separately for each isotope. This results in five (one for each run) times five (for each isotope) n -element ratio vectors:

$$L(x, b, i, t^i) = \begin{bmatrix} I[{}^i\text{Ar}(x, t_1^i) - {}^i\text{Ar}(b, t_1^i)] \\ I[{}^i\text{Ar}(x, t_2^i) - {}^i\text{Ar}(b, t_2^i)] \\ \vdots \\ I[{}^i\text{Ar}(x, t_n^i) - {}^i\text{Ar}(b, t_n^i)] \end{bmatrix} \quad (20)$$

These vectors are assembled into five $[n \times 5]$ matrices, each of which is partitioned into three groups according to the shared blank corrections:

$$G(i, t^i) = [L(u_1, b_1, i, t^i) L(s_1, b_1, i, t^i) | L(u_2, b_2, i, t^i) L(s_2, b_2, i, t^i) | L(s_3, b_3, i, t^i)] \\ = [g_1^i | g_2^i | g_3^i] \quad (21)$$

Joint regression to $t = 0$ yields a 5-element vector of log-intercepts for each isotope:

$$Z(i) = [Z(g_1, i) Z(g_2, i) Z(g_3, i)] \quad (22)$$

with $[5 \times 5]$ covariance matrices

$$\Sigma_{Z(i)} = \begin{bmatrix} \Sigma_{g_1}^i & 0_{2,2} & 0_{2,1} \\ 0_{2,2} & \Sigma_{g_2}^i & 0_{2,1} \\ 0_{1,2} & 0_{1,2} & \Sigma_{g_3}^i \end{bmatrix} \quad (23)$$

where $\Sigma_{g_j}^i$ is the covariance matrix of the j th group's ${}^i\text{Ar}$ intercepts. Next, we bring the ratio-intercept data for all five isotopes together into a single 25-element vector

$$Z = [Z(36) Z(37) Z(38) Z(39) Z(40)] \quad (24)$$

with $[25 \times 25]$ covariance matrix

$$\Sigma_Z = \begin{bmatrix} \Sigma_{Z(36)} & 0_{5,5} & 0_{5,5} & 0_{5,5} & 0_{5,5} \\ 0_{5,5} & \Sigma_{Z(37)} & 0_{5,5} & 0_{5,5} & 0_{5,5} \\ 0_{5,5} & 0_{5,5} & \Sigma_{Z(38)} & 0_{5,5} & 0_{5,5} \\ 0_{5,5} & 0_{5,5} & 0_{5,5} & \Sigma_{Z(39)} & 0_{5,5} \\ 0_{5,5} & 0_{5,5} & 0_{5,5} & 0_{5,5} & \Sigma_{Z(40)} \end{bmatrix} \quad (25)$$

Finally, we form 20 logratios with the following matrix operation:

$$X = Z J_X \quad (26)$$

The associated $[20 \times 20]$ covariance matrix is given by:

$$\Sigma_X = J_X' \Sigma_Z J_X \quad (27)$$

with J_X the $[25 \times 20]$ Jacobian matrix of the subtraction operation and J_X' its transpose:

$$J_X' = \begin{bmatrix} 1_{5,5} & 0_{5,5} & 0_{5,5} & 0_{5,5} & -1_{5,5} \\ 0_{5,5} & 1_{5,5} & 0_{5,5} & 0_{5,5} & -1_{5,5} \\ 0_{5,5} & 0_{5,5} & 1_{5,5} & 0_{5,5} & -1_{5,5} \\ 0_{5,5} & 0_{5,5} & 0_{5,5} & 1_{5,5} & -1_{5,5} \end{bmatrix} \quad (28)$$

where $1_{i,i}$ is an $[i \times i]$ identity matrix. We have now cast the raw mass spectrometer data in a common logratio format X (through either Eq. (17) or (26)) and associated covariance structure Σ_X (Eq. (18) or (27)). From here on, multicollector and peak-hopping data can be treated on an equal footing.

5. DETECTOR CALIBRATION

The different ion detectors in a multicollector mass spectrometer do not necessarily respond equally to ion beams of equal mass and size. The measured ratio of the beam intensities at $t = 0$ will therefore not necessarily equal the true isotopic ratio. This issue obviously does not occur in single collector instruments. Although the latest generation of multicollector noble gas mass spectrometers quantify the relative sensitivities internally through an electronic detector intercalibration, this section describes a data reduction protocol for a conventional ('analog') detector calibration.

Suppose that there are five detectors, one for each argon isotope, and denote these by $d[36]$, $d[37]$, $d[38]$, $d[39]$ and $d[40]$. The relative sensitivities of detectors $d[36]$ and $d[40]$ can be quantified by comparing the measured $^{40}\text{Ar}/^{36}\text{Ar}$ intensity ratio of an air shot with the known atmospheric ratio, as part of the mass fractionation correction (Section 6). The relative sensitivities of the remaining detectors, $d[37]$ – $d[40]$, on the other hand, are calibrated by steering a fixed ^{40}Ar beam from an air tank across them. The resulting signals of this ‘peak hopping’ experiment are extrapolated to $t = 0$ using the methods described in Section 4, resulting in four log-intercepts and their variances. No blank corrections are needed because we are only interested in the total amount of gas present in the mass spectrometer and not in the air composition itself. If the calibration experiment is repeated multiple times, then the measurements can be combined by taking the arithmetic mean of the logs (Section 13). To apply the detector calibration correction, we simply add the difference of the log-intercepts to the data, in matrix form. First, we append the log-intercepts of the calibration data to the sample vector.

$$X^* = [X \ Z(d[37]) \ Z(d[38]) \ Z(d[39]) \ Z(d[40])] \quad (29)$$

with $[24 \times 24]$ covariance matrix Σ_X^* :

$$\Sigma_X^* = \begin{bmatrix} \Sigma_X & 0_{20,1} & 0_{20,1} & 0_{20,1} & 0_{20,1} \\ 0_{1,20} & \sigma[Z(d[37])]^2 & 0 & 0 & 0 \\ 0_{1,20} & 0 & \sigma[Z(d[38])]^2 & 0 & 0 \\ 0_{1,20} & 0 & 0 & \sigma[Z(d[39])]^2 & 0 \\ 0_{1,20} & 0 & 0 & 0 & \sigma[Z(d[40])]^2 \end{bmatrix} \quad (30)$$

where X is a 20-element vector of sample and standard measurements (Eq. (17)) and Σ_X its covariance matrix (Eq. (18)), $Z(d[i])$ indicates the log intercept of ^{40}Ar measured by detector $d[i]$ at ‘time zero’, and $\sigma[Z(d[i])]$ is its standard error. Then the detector calibrated data (C) and their $[20 \times 20]$ covariance matrix (Σ_C) are obtained by:

$$C = X^* J_C \quad (31)$$

and

$$\Sigma_C = J_C^* \Sigma_X^* J_C \quad (32)$$

respectively, where J_C is the $[24 \times 20]$ Jacobian matrix of the detector calibration and J_C^* is its transpose:

$$J_C^* = \begin{bmatrix} 1_{4,4} & 0_{4,4} & 0_{4,4} & 0_{4,4} & 0_{4,4} & J_C^* \\ 0_{4,4} & 1_{4,4} & 0_{4,4} & 0_{4,4} & 0_{4,4} & J_C^* \\ 0_{4,4} & 0_{4,4} & 1_{4,4} & 0_{4,4} & 0_{4,4} & J_C^* \\ 0_{4,4} & 0_{4,4} & 0_{4,4} & 1_{4,4} & 0_{4,4} & J_C^* \\ 0_{4,4} & 0_{4,4} & 0_{4,4} & 0_{4,4} & 1_{4,4} & J_C^* \end{bmatrix} \quad (33)$$

with

$$J_C^* = \begin{bmatrix} 0 & 0 & 0 & 0 \\ -1 & 0 & 0 & 1 \\ 0 & -1 & 0 & 1 \\ 0 & 0 & -1 & 1 \end{bmatrix} \quad (34)$$

Note that, if all the measurements (samples, age standards and interference monitors) use the same detector calibration, then the associated analytical uncertainties cancel out in the age calculation (Section 12) and we can set $\sigma[Z(d[i])]^2 = 0 \ \forall i$ in Eq. (30).

6. MASS FRACTIONATION

The five argon isotopes of interest span a mass range of 10%. The sensitivity of both single- and multicollector instruments varies with atomic mass, and significant errors can occur if the resulting ‘mass fractionation’ is uncorrected for. The mass fractionation factor can be quantified by comparing the measured signal ratios of an air shot with its known isotopic ratio (298.56 ± 0.31 , Lee et al., 2006). For multicollector instruments, each detector has its own mass fractionation correction factor. For detectors $d[37]$, $d[38]$ and $d[39]$, these are obtained by peak hopping between masses 36 and 40. For $d[40]$ and $d[36]$, we can quantify the fractionation by directly monitoring the $^{36}\text{Ar}/^{40}\text{Ar}$ -ratio in multicollection mode. The exponential form of the kinetic isotope fractionation correction (Young et al., 2002) conveniently reduces to a linear equation in a logratio context:

$$l \left[\frac{^i\text{Ar}}{^j\text{Ar}} \right] = l \left[\frac{^i\text{Ar}[d[i]]}{^j\text{Ar}[d[j]]} \right] + \frac{l[i] - l[j]}{l[40] - l[36]} \left(A(j) + l \left[\frac{^{40}\text{Ar}}{^{36}\text{Ar}} \right]_a \right) \quad (35)$$

where $^i\text{Ar}[d[j]$ stands for the ^iAr signal measured on detector j and $A(j)$ is the ‘time zero’ intercept of $l \left[\frac{^{36}\text{Ar}[d[j]]}{^{40}\text{Ar}[d[j]]} \right]$, except if $j = 40$ on a multicollector instrument, in which case $A(j)$ is the ‘time zero’ intercept of $l \left[\frac{^{36}\text{Ar}[d[36]]}{^{40}\text{Ar}[d[40]]} \right]$. To apply Eq. (35), we append the air shot data and the true air ratio to the calibration-corrected logratio intercepts:

$$C^* = \left[C \ A(40) \ l \left[\frac{^{40}\text{Ar}}{^{36}\text{Ar}} \right]_a \right] \quad (36)$$

whose $[22 \times 22]$ covariance matrix Σ_C^* can be written as:

$$\Sigma_C^* = \begin{bmatrix} \Sigma_C & 0_{20,1} & 0_{20,1} \\ 0_{1,20} & \sigma[A(40)]^2 & 0 \\ 0_{1,20} & 0 & 0 \end{bmatrix} \quad (37)$$

Note that Eq. (37) does not specify the analytical uncertainty of the atmospheric reference ratio. This is because any uncertainty resulting from an incorrect air-ratio at this point will cancel out during the atmospheric argon correction (Section 10). Recasting Eq. (35) in matrix form, the fractionation correction of the sample and fluence measurements can be written as:

$$F = C^* J_F \quad (38)$$

with $[20 \times 20]$ covariance matrix

$$\Sigma_F = J_F^* \Sigma_C^* J_F \quad (39)$$

where J_F is the $[22 \times 20]$ Jacobian matrix of the mass fractionation correction and J_F^* is its transpose:

$$J'_F = \begin{bmatrix} 1_{4,4} & 0_{4,4} & 0_{4,4} & 0_{4,4} & 0_{4,4} & J_F^* \\ 0_{4,4} & 1_{4,4} & 0_{4,4} & 0_{4,4} & 0_{4,4} & J_F^* \\ 0_{4,4} & 0_{4,4} & 1_{4,4} & 0_{4,4} & 0_{4,4} & J_F^* \\ 0_{4,4} & 0_{4,4} & 0_{4,4} & 1_{4,4} & 0_{4,4} & J_F^* \\ 0_{4,4} & 0_{4,4} & 0_{4,4} & 0_{4,4} & 1_{4,4} & J_F^* \end{bmatrix} \quad (40)$$

with

$$J_F^* = \begin{bmatrix} -1.000 & -1.000 \\ -0.740 & -0.740 \\ -0.487 & -0.487 \\ -0.240 & -0.240 \end{bmatrix} \quad (41)$$

7. DECAY CORRECTIONS

Two of the five argon isotopes of interest are radioactive: ^{37}Ar ($t_{1/2} = 34.95 \pm 0.08$ days, [Renne and Norman, 2001](#)) and ^{39}Ar ($t_{1/2} = 269 \pm 3$ years, [Stoener et al., 1965](#)). A correction is required for the loss of these isotopes during the time elapsed between irradiation and analysis:

$$I^i[\text{Ar}]_0 = I^i[\text{Ar}](\tau) + r(\lambda_i, \tau) \quad (42)$$

where $I^i[\text{Ar}]_0$ is the total amount of isotope i formed during irradiation, $I^i[\text{Ar}](\tau)$ is the amount remaining at a time τ after the end of the irradiation and $r(\lambda_i, \tau)$ is the amount lost due to radioactivity when the decay constant is λ_i . Using a similar approach to [Wijbrans and McDougall \(1986\)](#), $r(\lambda_i, \tau)$ can be calculated as:

$$r(\lambda_i, \tau) = I \left[\sum_j P_j \Delta t_j \right] - I \left[\sum_j \frac{P_j}{\lambda_i} \left(\frac{1}{e^{\lambda_i \Delta \tau_j}} - \frac{1}{e^{\lambda_i [\Delta \tau_j + \Delta t_j]}} \right) \right] \quad (43)$$

where P_j is the power and Δt_j the duration of the j th irradiation interval and $\Delta \tau_j$ is the time elapsed between the end of the j th irradiation segment and τ . At this point it is important to merge the data reduction pathways for the samples and fluence monitors with those of any co-irradiated K-glass and Ca-salt. This is because they are all affected by the same decay constant uncertainties, resulting in correlated errors. However, in this Section we will, for the sake of simplicity, assume that $[^{36}\text{Ar}/^{37}\text{Ar}]_{ca}$, $[^{39}\text{Ar}/^{37}\text{Ar}]_{ca}$ and $[^{39}\text{Ar}/^{40}\text{Ar}]_k$ have been obtained from elsewhere and do not need to be corrected for radioactive decay. For completeness, further details about the joint analysis of co-irradiated interference monitors with the sample are given in [Appendix A](#). To apply the decay correction to the samples and fluence monitors, we first concatenate all the decay corrections into one 5-element vector:

$$r(i) = [r(\lambda_i, \tau[u_1]) \quad r(\lambda_i, \tau[s_1]) \quad r(\lambda_i, \tau[u_2]) \quad r(\lambda_i, \tau[s_2]) \quad r(\lambda_i, \tau[s_3])] \quad (44)$$

The $[5 \times 5]$ covariance matrix of which is given by:

$$\Sigma_{r(i)} = J'_{r(i)} \sigma(\lambda_i)^2 J_{r(i)} \quad (45)$$

where $\sigma(\lambda_i)$ is the standard error of the ^iAr decay constant, and $J_{r(i)}$ is the Jacobian matrix:

$$J_r = \begin{bmatrix} \frac{\partial r(\lambda_i, \tau[u_1])}{\partial \lambda_i} & \frac{\partial r(\lambda_i, \tau[s_1])}{\partial \lambda_i} & \frac{\partial r(\lambda_i, \tau[u_2])}{\partial \lambda_i} & \frac{\partial r(\lambda_i, \tau[s_2])}{\partial \lambda_i} & \frac{\partial r(\lambda_i, \tau[s_3])}{\partial \lambda_i} \end{bmatrix} \quad (46)$$

with the partial derivatives given by:

$$\frac{\partial r(\lambda_i, \tau[x])}{\partial \lambda_i} = \sum_j \frac{P_j}{\lambda_i} \left[\frac{1 + \lambda_i \Delta \tau_j[x]}{e^{\lambda_i \Delta \tau_j[x]}} - \frac{1 + \lambda_i (\Delta \tau_j[x] + \Delta t_j)}{e^{\lambda_i (\Delta \tau_j[x] + \Delta t_j)}} \right] \quad (47)$$

Next, we append the vector of 10 decay corrections to the 20 fractionation-corrected logratio intercepts:

$$F^* = [F \quad r(37) \quad r(39)] \quad (48)$$

with $[30 \times 30]$ covariance matrix

$$\Sigma_{F^*} = \begin{bmatrix} \Sigma_F & 0_{20,5} & 0_{20,5} \\ 0_{5,20} & \Sigma_{r(37)} & 0 \\ 0_{5,20} & 0 & \Sigma_{r(39)} \end{bmatrix} \quad (49)$$

The decay correction can then be cast into matrix form as

$$D = F^* J_D \quad (50)$$

yielding a 20-element vector with covariance matrix

$$\Sigma_D = J'_D \Sigma_{F^*} J_D \quad (51)$$

using the $[30 \times 20]$ Jacobian matrix J_D and its transpose J'_D :

$$J'_D = [1_{20,20} \quad J_{D(37)}^* \quad J_{D(39)}^*] \quad (52)$$

with

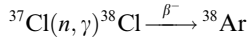
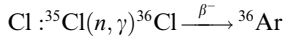
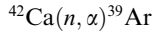
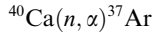
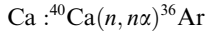
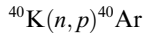
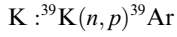
$$J_{D(i)}^* = \begin{bmatrix} J_{D(i)}^{**} & 0_{4,1} & 0_{4,1} & 0_{4,1} & 0_{4,1} \\ 0_{4,1} & J_{D(i)}^{**} & 0_{4,1} & 0_{4,1} & 0_{4,1} \\ 0_{4,1} & 0_{4,1} & J_{D(i)}^{**} & 0_{4,1} & 0_{4,1} \\ 0_{4,1} & 0_{4,1} & 0_{4,1} & J_{D(i)}^{**} & 0_{4,1} \\ 0_{4,1} & 0_{4,1} & 0_{4,1} & 0_{4,1} & J_{D(i)}^{**} \end{bmatrix} \quad (53)$$

where

$$J_{D(37)}^{**} = \begin{bmatrix} 0 \\ 1 \\ 0 \\ 0 \end{bmatrix} \quad \text{and} \quad J_{D(39)}^{**} = \begin{bmatrix} 0 \\ 0 \\ 0 \\ 1 \end{bmatrix} \quad (54)$$

8. INTERFERENCE CORRECTIONS

The $^{40}\text{Ar}/^{39}\text{Ar}$ -method pairs the natural radioactive decay of ^{40}K to ^{40}Ar with the synthetic activation of ^{39}K to ^{39}Ar . Unfortunately, neutron activation produces not only ^{39}Ar but a host of other Ar-isotopes as well. The most important reactions are [McDougall and Harrison \(1999\)](#):



The first five of these reactions can be characterised by mass spectrometric analysis of K-glass (${}^{40}\text{Ar}/{}^{39}\text{Ar}$ ratio) and Ca-salt (${}^{36}\text{Ar}/{}^{37}\text{Ar}$ and ${}^{39}\text{Ar}/{}^{37}\text{Ar}$ ratios). These ratios are directly incorporated into Eq. (5) (parameters a , b and f). The chlorine decay products, on the other hand, are generally calculated from the independently determined and reactor-specific ${}^{36}\text{Cl}/{}^{38}\text{Cl}$ -production ratio and will be discussed in Section 9. If the K- and Ca-interference corrections are based on externally determined values, then we compile these with the decay-corrected sample and fluence measurements for further processing in Section 10:

$$I = [D \ D(ca) \ D(k)] \quad (55)$$

where, using the notation of Section 7, $D(ca)$ is a 2-element vector containing the decay-corrected ${}^{36}\text{Ar}/{}^{37}\text{Ar}$ - and ${}^{39}\text{Ar}/{}^{37}\text{Ar}$ -logratios of neutron-activated Ca, and $D(k)$ is the ${}^{40}\text{Ar}/{}^{39}\text{Ar}$ -logratio of neutron-activated K. The corresponding $[23 \times 23]$ covariance matrix is given by

$$\Sigma_I = \begin{bmatrix} \Sigma_D & 0_{20,2} & 0_{20,1} \\ 0_{2,20} & \Sigma_{D(ca)} & 0_{2,1} \\ 0_{1,20} & 0_{1,2} & \sigma_{D(k)}^2 \end{bmatrix} \quad (56)$$

After which we can proceed to Section 9 of this paper. If, on the other hand, Ca and K interferences are quantified by co-irradiated Ca-salts and K-glass, then we can explicitly include the resulting mass spectrometer uncertainties into the error propagation. Further details of this are provided in Appendix A. In summary, the vector I , obtained from either Eq. (55) or Appendix A, contains all the information required to solve Eq. (5) except for factor ‘ c ’, which is discussed next.

9. CL-DECAY

In contrast with the K- and Ca-interferences, which can be directly characterised by mass spectrometric analysis of co-irradiated materials, the Cl-interference on ${}^{36}\text{Ar}$ is generally calculated from an independently determined and reactor-specific ${}^{36}\text{Cl}/{}^{38}\text{Cl}$ -production ratio (Foland et al., 1993; Renne et al., 2008). Let $G(x)$ be the logratio of the chlorine decay products (i.e., $I[{}^{36}\text{Ar}/{}^{38}\text{Ar}]$) in sample (or fluence monitor) x . Using the approach of Wijbrans and McDougall (1986) to account for the radioactive decay of Cl to Ar, we obtain:

$$G(x) = I \left[\frac{{}^{36}\text{Cl}}{{}^{38}\text{Cl}} \right] + g(\tau[x]) \quad (57)$$

with

$$g(\tau) = I \left[1 + \frac{\sum_j P_j (e^{-\lambda_{36}(\Delta\tau_j + \Delta\tau_j)} - e^{-\lambda_{36}\Delta\tau_j})}{\lambda_{36} \sum_j P_j \Delta\tau_j} \right] \quad (58)$$

where λ_{36} is the ${}^{36}\text{Cl}$ decay constant and τ , $\Delta\tau_i$ and $\Delta\tau_j$ are as defined in Section 7. The decay corrections can be compiled into a single five-element vector

$$G = [G(u_1) \ G(s_1) \ G(u_2) \ G(s_2) \ G(s_3)] \quad (59)$$

whose $[5 \times 5]$ covariance matrix is given by:

$$\Sigma_G = J'_G \begin{bmatrix} \sigma \left(I \left[\frac{{}^{36}\text{Cl}}{{}^{38}\text{Cl}} \right] \right)^2 & 0 \\ 0 & \sigma(\lambda_{36})^2 \end{bmatrix} J_G \quad (60)$$

with

$$J_G = \begin{bmatrix} 1 & 1 & 1 & 1 & 1 \\ \partial G(u_1)/\partial \lambda_{36} & \partial G(s_1)/\partial \lambda_{36} & \partial G(u_2)/\partial \lambda_{36} & \partial G(s_2)/\partial \lambda_{36} & \partial G(s_3)/\partial \lambda_{36} \end{bmatrix} \quad (61)$$

where the partial derivatives are given by:

$$\frac{\partial G(x)}{\partial \lambda_{36}} = \frac{\sum_j P_j [(1 + \lambda_{36} \Delta\tau_j[x]) e^{-\lambda_{36} \Delta\tau_j} - (1 + \lambda_{36} [\Delta\tau_j[x] + \Delta\tau_j]) e^{-\lambda_{36} (\Delta\tau_j[x] + \Delta\tau_j)}]}{\lambda_{36} \sum_j P_j [\lambda_{36} \Delta\tau_j + e^{-\lambda_{36} (\Delta\tau_j[x] + \Delta\tau_j)} - e^{-\lambda_{36} \Delta\tau_j[x]}]} \quad (62)$$

Note that the Cl-interference correction implemented in Eq. (8) does not account for the presence of atmospheric ${}^{38}\text{Ar}$ and the production of ${}^{38}\text{Ar}$ from K. Doing so is straightforward but adds considerably more complexity to Eq. (5) (Appendix B).

10. ${}^{40}\text{Ar}^*/{}^{39}\text{Ar}_K$

After all the preprocessing discussed in the previous sections, we have finally gathered all the ratios required to solve Eq. (5). To this end, we compile all the information obtained thus far into a single vector of logratios

$$U = \left[I \ I \left[\frac{{}^{40}\text{Ar}}{{}^{36}\text{Ar}} \right]_a \ G \right] \quad (63)$$

and its $[29 \times 29]$ covariance matrix

$$\Sigma_U = \begin{bmatrix} \Sigma_I & 0_{23,1} & 0_{23,5} \\ 0_{1,23} & \sigma \left(I \left[\frac{{}^{40}\text{Ar}}{{}^{36}\text{Ar}} \right]_a \right)^2 & 0_{1,5} \\ 0_{5,23} & 0_{5,1} & \Sigma_G \end{bmatrix} \quad (64)$$

To simplify the notation in the remainder of this Section, it is useful to permute U and Σ_U so that the Cl-interference data (G) are interspersed with the samples and fluence monitors:

$$U^* = UP \quad \text{and} \quad \Sigma_U^* = PUP \quad (65)$$

where P is the $[29 \times 29]$ permutation matrix

$$P = \begin{bmatrix} 1_{4,4} & 0_{4,1} & 0_{4,4} & 0_{4,1} & 0_{4,4} & 0_{4,1} & 0_{4,4} & 0_{4,1} & 0_{4,4} & 0_{4,1} & 0_{4,4} \\ 0_{4,4} & 0_{4,1} & 1_{4,4} & 0_{4,1} & 0_{4,4} & 0_{4,1} & 0_{4,4} & 0_{4,1} & 0_{4,4} & 0_{4,1} & 0_{4,4} \\ 0_{4,4} & 0_{4,1} & 0_{4,4} & 0_{4,1} & 1_{4,4} & 0_{4,1} & 0_{4,4} & 0_{4,1} & 0_{4,4} & 0_{4,1} & 0_{4,4} \\ 0_{4,4} & 0_{4,1} & 0_{4,4} & 0_{4,1} & 0_{4,4} & 0_{4,1} & 1_{4,4} & 0_{4,1} & 0_{4,4} & 0_{4,1} & 0_{4,4} \\ 0_{4,4} & 0_{4,1} & 0_{4,4} & 0_{4,1} & 0_{4,4} & 0_{4,1} & 0_{4,4} & 0_{4,1} & 1_{4,4} & 0_{4,1} & 0_{4,4} \\ 0_{4,4} & 0_{4,1} & 0_{4,4} & 0_{4,1} & 0_{4,4} & 0_{4,1} & 0_{4,4} & 0_{4,1} & 0_{4,4} & 0_{4,1} & 1_{4,4} \\ 0_{1,4} & 1 & 0_{1,4} & 0 & 0_{1,4} & 0 & 0_{1,4} & 0 & 0_{1,4} & 0 & 0_{1,4} \\ 0_{1,4} & 0 & 0_{1,4} & 1 & 0_{1,4} & 0 & 0_{1,4} & 0 & 0_{1,4} & 0 & 0_{1,4} \\ 0_{1,4} & 0 & 0_{1,4} & 0 & 0_{1,4} & 1 & 0_{1,4} & 0 & 0_{1,4} & 0 & 0_{1,4} \\ 0_{1,4} & 0 & 0_{1,4} & 0 & 0_{1,4} & 0 & 0_{1,4} & 1 & 0_{1,4} & 0 & 0_{1,4} \\ 0_{1,4} & 0 & 0_{1,4} & 0 & 0_{1,4} & 0 & 0_{1,4} & 0 & 0_{1,4} & 1 & 0_{1,4} \end{bmatrix} \quad (66)$$

Next we convert the logratio vector U^* into a vector of 30 ratios

$$W = [V(u_1)V(s_1)V(u_2)V(s_2)V(s_3)] \quad (67)$$

where

$$V(x) = [a(x) \ b(x) \ c(x) \ d(x) \ e(x) \ f(x)] \quad (68)$$

with a – f as defined in Eqs. (6)–(11). $f(x)$ is the same for all analyses in this example but may vary between samples when combining different irradiations. W is calculated in matrix form by

$$W = \exp[U^* J_V] \quad (69)$$

with J_V the $[29 \times 30]$ Jacobian matrix:

$$J_V = \begin{bmatrix} J_V^* & 0_{5,6} & 0_{5,6} & 0_{5,6} & 0_{5,6} \\ 0_{5,6} & J_V^* & 0_{5,6} & 0_{5,6} & 0_{5,6} \\ 0_{5,6} & 0_{5,6} & J_V^* & 0_{5,6} & 0_{5,6} \\ 0_{5,6} & 0_{5,6} & 0_{5,6} & J_V^* & 0_{5,6} \\ 0_{5,6} & 0_{5,6} & 0_{5,6} & 0_{5,6} & J_V^* \\ J_V^{**} & J_V^{**} & J_V^{**} & J_V^{**} & J_V^{**} \end{bmatrix} \quad (70)$$

where

$$J_V^* = \begin{bmatrix} 1 & 0 & 0 & 0 & 0 & 0 \\ 0 & 1 & 0 & 0 & 1 & 0 \\ 0 & 0 & 1 & 0 & 0 & 0 \\ 0 & 0 & 0 & 1 & 0 & 0 \\ 0 & 0 & 1 & 0 & 0 & 0 \end{bmatrix} \quad \text{and} \quad J_V^{**} = \begin{bmatrix} 0 & 1 & 0 & 0 & 0 & 0 \\ 0 & 0 & 0 & 0 & 1 & 0 \\ 0 & 0 & 0 & 0 & 0 & 1 \\ 1 & 1 & 1 & 0 & 0 & 0 \end{bmatrix} \quad (71)$$

The $[30 \times 30]$ covariance matrix of W is obtained by

$$\Sigma_W = J_W' \Sigma_U J_W \quad (72)$$

where the $[29 \times 30]$ Jacobian J_W is given by

$$J_W = \begin{bmatrix} J_W^* & 0_{5,6} & 0_{5,6} & 0_{5,6} & 0_{5,6} \\ 0_{5,6} & J_W^* & 0_{5,6} & 0_{5,6} & 0_{5,6} \\ 0_{5,6} & 0_{5,6} & J_W^* & 0_{5,6} & 0_{5,6} \\ 0_{5,6} & 0_{5,6} & 0_{5,6} & J_W^* & 0_{5,6} \\ 0_{5,6} & 0_{5,6} & 0_{5,6} & 0_{5,6} & J_W^* \\ J_W^{**} & J_W^{**} & J_W^{**} & J_W^{**} & J_W^{**} \end{bmatrix} \quad (73)$$

with

$$J_W^* = \begin{bmatrix} a & 0 & 0 & 0 & 0 & 0 \\ 0 & b & 0 & 0 & e & 0 \\ 0 & 0 & c & 0 & 0 & 0 \\ 0 & 0 & 0 & d & 0 & 0 \\ 0 & 0 & c & 0 & 0 & 0 \end{bmatrix} \quad \text{and} \quad J_W^{**} = \begin{bmatrix} 0 & b & 0 & 0 & 0 & 0 \\ 0 & 0 & 0 & 0 & e & 0 \\ 0 & 0 & 0 & 0 & 0 & f \\ a & b & c & 0 & 0 & 0 \end{bmatrix} \quad (74)$$

The five element vector R of $^{40}\text{Ar}^*/^{39}\text{Ar}_K$ -ratios is calculated with Eq. (5):

$$R = [R(u_1) \ R(s_1) \ R(u_2) \ R(s_2) \ R(s_3)] \quad (75)$$

and its $[5 \times 5]$ covariance matrix is obtained by

$$\Sigma_R = J_R' \Sigma_W J_R \quad (76)$$

where J_R is the $[30 \times 5]$ Jacobian matrix

$$J_R = \begin{bmatrix} J_R^*(u_1) & 0_{6,1} & 0_{6,1} & 0_{6,1} & 0_{6,1} \\ 0_{6,1} & J_R^*(s_1) & 0_{6,1} & 0_{6,1} & 0_{6,1} \\ 0_{6,1} & 0_{6,1} & J_R^*(u_2) & 0_{6,1} & 0_{6,1} \\ 0_{6,1} & 0_{6,1} & 0_{6,1} & J_R^*(s_2) & 0_{6,1} \\ 0_{6,1} & 0_{6,1} & 0_{6,1} & 0_{6,1} & J_R^*(s_3) \end{bmatrix} \quad (77)$$

with

$$J_R^*(x) = \begin{bmatrix} -1 \\ \frac{d(x) - e(x)}{1} \\ \frac{d(x) - e(x)}{1} \\ \frac{d(x) - e(x)}{1} \\ \frac{a(x) - b(x) - c(x) - 1}{[d(x) - e(x)]^2} \\ \frac{1 - a(x) + b(x) + c(x)}{[d(x) - e(x)]^2} \\ -1 \end{bmatrix} \quad (78)$$

11. J-FACTORS

The parameter J quantifying the production of ^{39}Ar from ^{39}K in the age equation is determined by analysing the argon composition of a co-irradiated fluence monitor with accurately known K–Ar age (T_s). This composition may vary across the irradiation stack due to neutron flux gradients in the reactor, which can be quantified by analysing several fluence monitors interspersed with the samples at known positions. The most appropriate J-factor for each sample is then obtained by simple linear interpolation:

$$J(x) = \frac{e^{\lambda_{40} T_s} - 1}{R(s|x)} \quad (79)$$

where $R(s|x)$ denotes the $^{40}\text{Ar}^*/^{39}\text{Ar}_K$ -ratio of the fluence monitors interpolated to the position of sample x (which is henceforth referred to as $p[x]$). Applying this procedure to our two sample – three monitor case study, we form a four-element vector of sample ratios and interpolated fluence monitor ratios:

$$Y = [R(u_1) \ R(u_2) \ R(s|u_1) \ R(s|u_2)] = R J_Y \quad (80)$$

with $[4 \times 4]$ covariance matrix

$$\Sigma_Y = J'_Y \Sigma_R J_Y \quad (81)$$

where R is the vector of $^{40}\text{Ar}^*/^{39}\text{Ar}_K$ -ratios for the samples and fluence monitors (Eq. (75)), J_Y is the $[5 \times 4]$ Jacobian matrix and J'_Y is its transpose. Suppose that sample u_1 sits between monitors s_1 and s_2 in the irradiation stack, and u_2 sits between monitors s_2 and s_3 . Then

$$J'_Y = \begin{bmatrix} 1 & 0 & 0 & 0 & 0 \\ 0 & 0 & 1 & 0 & 0 \\ 0 & \frac{p[u_1]-p[s_1]}{p[s_2]-p[s_1]} & 0 & \frac{p[s_2]-p[u_1]}{p[s_2]-p[s_1]} & 0 \\ 0 & 0 & 0 & \frac{p[u_2]-p[s_2]}{p[s_3]-p[s_2]} & \frac{p[s_3]-p[u_2]}{p[s_3]-p[s_2]} \end{bmatrix} \quad (82)$$

Finally, we use Eq. (79) to generate a five-element vector of sample $^{40}\text{Ar}^*/^{39}\text{Ar}_K$ -ratios, their respective J -factors, and the ^{40}K decay constant:

$$Q = [R(u_1) \ R(u_2) \ J(u_1) \ J(u_2) \ \lambda_{40}] \quad (83)$$

with $[5 \times 5]$ covariance matrix

$$\Sigma_Q = J'_Q \begin{bmatrix} \Sigma_Y & 0 & 0 \\ 0 & \sigma^2(\lambda_{40}) & 0 \\ 0 & 0 & \sigma^2(T_s) \end{bmatrix} J_Q \quad (84)$$

where J_Q is the $[6 \times 5]$ Jacobian matrix and J'_Q is its transpose:

$$J'_Q = \begin{bmatrix} 1 & 0 & 0 & 0 & 0 & 0 \\ 0 & 1 & 0 & 0 & 0 & 0 \\ 0 & 0 & \frac{1-e^{40T_s}}{R(s|u_1)^2} & 0 & \frac{T_s e^{40T_s}}{R(s|u_1)} & \frac{\lambda_{40} e^{40T_s}}{R(s|u_1)} \\ 0 & 0 & 0 & \frac{1-e^{40T_s}}{R(s|u_2)^2} & \frac{T_s e^{40T_s}}{R(s|u_2)} & \frac{\lambda_{40} e^{40T_s}}{R(s|u_2)} \\ 0 & 0 & 0 & 0 & 1 & 0 \end{bmatrix} \quad (85)$$

The decay constant λ_{40} is included into Eq. (83) because this parameter appears in both the expression for J (Eq. (79)) and the age equation (Eq. 3), resulting in correlated errors.

12. SOLVING THE AGE EQUATION

The $^{40}\text{Ar}/^{39}\text{Ar}$ -ages of samples u_1 and u_2 are calculated by plugging the relevant items of vector Q into Eq. (3), resulting in a 2-element vector T

$$T = [T(u_1) \ T(u_2)] \quad (86)$$

with $[2 \times 2]$ covariance matrix

$$\Sigma_T = J'_T \Sigma_Q J_T \quad (87)$$

where J_T is the $[5 \times 2]$ Jacobian matrix:

$$J_T = \begin{bmatrix} \frac{J(u_1)}{\lambda_{40}[1+J(u_1)R(u_1)]} & 0 \\ 0 & \frac{J(u_2)}{\lambda_{40}[1+J(u_2)R(u_2)]} \\ \frac{R(u_1)}{\lambda_{40}[1+J(u_1)R(u_1)]} & 0 \\ 0 & \frac{R(u_2)}{\lambda_{40}[1+J(u_2)R(u_2)]} \\ -\frac{[1+J(u_1)R(u_1)]}{\lambda_{40}^2} & -\frac{[1+J(u_2)R(u_2)]}{\lambda_{40}^2} \end{bmatrix} \quad (88)$$

13. (WEIGHTED) MEAN AGES

Given a vector of N age measurements ($T = [T(u_1) \ T(u_2) \ \dots \ T(u_N)]$), we can calculate the arithmetic mean age \bar{T}_a as:

$$\bar{T}_a = (T \mathbf{1}_{N,1})/N \quad (89)$$

with standard error

$$\sigma^2(\bar{T}_a) = (\mathbf{1}_{1,N} \Sigma_T \mathbf{1}_{N,1})/N \quad (90)$$

Alternatively, to calculate the error-weighted mean \bar{T}_w , first calculate its variance:

$$\sigma^2(\bar{T}_w) = (\mathbf{1}_{1,N} \Sigma_T^{-1} \mathbf{1}_{N,1})^{-1} \quad (91)$$

then

$$\bar{T}_w = \sigma^2(\bar{T}_w) (T \Sigma_T^{-1} \mathbf{1}_{N,1}) \quad (92)$$

The MSWD ('Mean Square of the Weighted Deviates', also known as 'reduced Chi-square statistic' outside geology) is a measure of the ratio of the observed scatter of the data points ($T[u_i]$) around the mean value (\bar{T}) to the expected scatter from the assigned errors (Σ_T):

$$MSWD = \frac{1}{N-1} [T - \bar{T}] \Sigma_T^{-1} [T - \bar{T}]' \quad (93)$$

If $MSWD > 1$, then the samples are said to be 'overdispersed' with respect to the analytical uncertainty. This commonly occurs in very precise datasets, which have sufficient power to resolve minute levels of sample heterogeneity. In this case, the geologically meaningful levels of heterogeneity can be quantified using a 'mixed effects' model with two sources of analytical uncertainty:

$$T[u_i] \sim \mathcal{N}[\bar{T}, \sigma(T[u_i])^2 + \zeta^2] \quad (94)$$

where $\mathcal{N}[a,b]$ stands for "the Normal distribution with mean a and variance b ", and ζ^2 is the 'overdispersion' (Vermeesch, 2010). Eq. (94) can be solved by the method of maximum likelihood, which simultaneously estimates the average, its standard error, and the overdispersion.

14. AR-AR_REDUX

The revised data reduction procedure outlined in this paper revisits every aspect of the $^{40}\text{Ar}/^{39}\text{Ar}$ method. Unfortunately, the matrix format of the calculations is incompatible with existing data reduction platforms such as `ArArCalc` (Koppers, 2002). A new computer code named `Ar-Ar_Redux` was developed to solve this problem and facilitate the adoption of the methods described herein. A prototype version of `Ar-Ar_Redux` currently exists as a package in the R programming environment, which is an increasingly popular open source alternative to `Matlab`, available free of charge on any operating system at <http://r-project.org>. A standalone program with graphical user interface is in development for future release. 'Ar-Ar_Redux' derives its name from 'U-Pb_Redux', which is a similar program developed by the U-Pb dating community (McLean et al., 2011; Bowring et al., 2011). Both programs use a similar matrix formulation and, although `U-Pb_Redux` currently does not employ a logratio

transformation, future versions of it will. The R-version of Ar-Ar_Redux can be downloaded free of charge from the ‘Comprehensive R-Archive Network’ (CRAN, <http://cran.r-project.org>). Appendix C gives a brief introduction to Ar-Ar_Redux, with further details provided at <http://redux.london-geochron.com>. The latter website will also host the standalone version of the program when it is ready for public release. Currently, Ar-Ar_Redux accepts input files that are compatible with the ARGUS-VI multicollector instrument, but other input formats can easily be implemented as well. Ar-Ar_Redux is intended to be a community-driven software platform, which can evolve to accommodate the demands and expectations of $^{40}\text{Ar}/^{39}\text{Ar}$ practitioners, and the reader is invited to contact the author with any questions or requests. The program is bundled with a real dataset, which was kindly provided by Prof. David Phillips of the University of Melbourne.

15. DISCUSSION AND CONCLUSIONS

One might wonder how much difference the revised data reduction workflow makes compared to currently used procedures. The answer to this question depends on the particular details of the sample of interest. For example:

- Error correlations are stronger when several samples share the same blank than when each sample has its own blank.
- Large interference corrections result in strong error correlations.
- Multicollector data are more strongly correlated than ‘peak hopping’ data.
- Analysing co-irradiated interference monitors yields stronger error correlations than using externally provided interference corrections.

Regarding the latter two examples, it is important to note that correlated errors should not necessarily be considered undesirable, as long as they are properly quantified. It is only when covariances are ignored that uncertainties are overestimated, potentially significant age differences are blurred out and geologically meaningful information is lost. Experience tells that the covariance terms can be very substantial. For the test data provided with Ar-Ar_Redux, error correlations (defined as $\rho(x, y) = \text{cov}(x, y) / [\sigma(x)\sigma(y)]$) between aliquots of the same sample are on the order of 0.9.

Renne et al. (1998) make the distinction between ‘internal’ and ‘external’ errors. ‘internal errors’ can be conceptually defined as the natural variability that would arise if the same sample were dated multiple times under the same experimental conditions. ‘external’ errors include the systematic effects of decay constant uncertainty, the K/Ar ratio of the age standard, the air ratio etc. Renne et al. (1998) point out that “comparison of two different $^{40}\text{Ar}/^{39}\text{Ar}$ dates based on the same standard may legitimately ignore uncertainties in K–Ar data, decay constants, as well as all intercalibration factors common to both dates”. However, when comparing a $^{40}\text{Ar}/^{39}\text{Ar}$ -age with, say, a zircon U/Pb age, “it is important to consider all sources of systematic error in data from both radioisotopic

systems”. Thus, great care must be taken which sources of uncertainty should or should not be included in the error propagation. In practical terms, this results in different analytical forms of the error propagation depending on the situation. This added complexity disappears entirely when using the methods presented in this paper. By processing the data in matrix form and explicitly taking into account covariances, the internal and external errors are jointly considered, with the latter corresponding to the off-diagonal terms of the covariance matrix. Revisiting Renne et al. (1998)’s two scenarios, we find that the difference between two $^{40}\text{Ar}/^{39}\text{Ar}$ dates based on the same standard may appear to be statistically insignificant compared to their respective variances, but statistically significant when the covariance terms are considered (Fig. 2).

This paper has revisited many but not all aspects of $^{40}\text{Ar}/^{39}\text{Ar}$ data reduction. For example, it has not discussed isochrons, in which linear regression is used to deconvolve the radiogenic and inherited argon components without the need to assume an atmospheric composition for the latter. Although the least squares algorithms which are currently used for this purpose do take into account error correlations between the x - and y -variables (e.g., York, 1968), they ignore the covariance between different samples. Similarly, thermal modelling is done by jointly considering multiple analyses and finding best-fitting (‘Arrhenius’) trends to them. Current fitting algorithms do not account for the significant error correlations that exist between subsequent heating steps in a diffusion experiment. The covariant structure of linear regression naturally follows from the covariant age structure represented by Eqs. (86) and (87), but a detailed discussion of this will be deferred to a forthcoming publication.

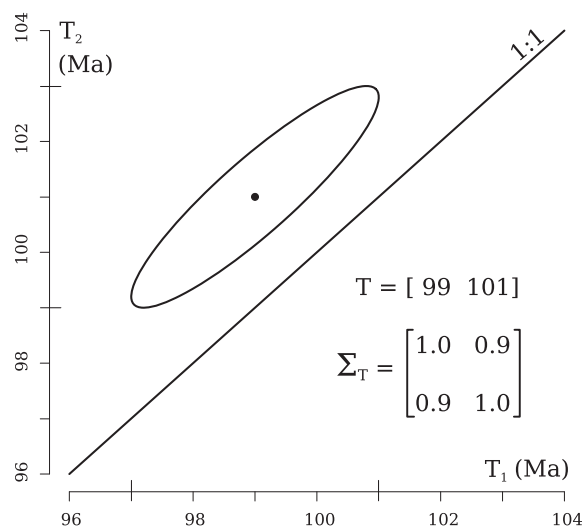


Fig. 2. A synthetic yet realistic example of two replicate age estimates of the same sample ($T_1 = 99$ Ma and $T_2 = 101$ Ma) plotted against each other as an error ellipse. Ignoring the covariances, the two dates appear to agree within two standard errors. Taking into account the off-diagonal terms of the covariance matrix (Σ_T), however, reveals that the two samples are overdispersed with respect to the analytical uncertainties.

In summary, this paper presented a fresh look at the $^{40}\text{Ar}/^{39}\text{Ar}$ method, by recasting every aspect of it into a matrix form and rigorously keeping track of all covariances. Thus, the methods outlined in this paper put the $^{40}\text{Ar}/^{39}\text{Ar}$ method on an equal footing with the U–Pb method (McLean et al., 2011). Using the same data reduction framework for both methods will improve their intercomparability, which in turn will benefit the accuracy and precision of the geologic time scale (Min et al., 2000; Kuiper et al., 2008).

ACKNOWLEDGMENTS

The author would like to thank David Phillips and Erin Matchan (Melbourne) for providing pilot data which have greatly accelerated the development of Ar–Ar_Redux. The manuscript benefited from discussions with James Schwanethal and Noah McLean, and constructive reviews by Chris Hall and three anonymous reviewers. The research leading to these results has received funding from the European Research Council under the European Union's Seventh Framework Programme (FP7/2007-2013)/ERC Grant agreement n°259504 ('KARSD').

APPENDIX A. CALCULATION OF INTERFERENCE CORRECTIONS BY MASS SPECTROMETRIC ANALYSIS OF CO-IRRADIATED MONITOR MATERIALS

Neutron reactions on Ca produce interferences on ^{36}Ar and ^{39}Ar , which can be corrected for by monitoring the $^{36}\text{Ar}/^{37}\text{Ar}$ - and $^{39}\text{Ar}/^{37}\text{Ar}$ -ratios of co-irradiated Ca-salts (Section 8). In this Section, we will use the same simplified regression methods as in Sections 3 and 4. If the three Ar-isotopes of interest are measured in multicollector mode, then their time resolved and blank corrected signals can be cast into the following $[n \times 2]$ logratio matrix:

$$L(ca, b, t) = \begin{bmatrix} I \left[\frac{^{36}\text{Ar}^b(ca, t_1)}{^{37}\text{Ar}^b(ca, t_1)} \right] & I \left[\frac{^{39}\text{Ar}^b(ca, t_1)}{^{37}\text{Ar}^b(ca, t_1)} \right] \\ I \left[\frac{^{36}\text{Ar}^b(ca, t_2)}{^{37}\text{Ar}^b(ca, t_2)} \right] & I \left[\frac{^{39}\text{Ar}^b(ca, t_2)}{^{37}\text{Ar}^b(ca, t_2)} \right] \\ \vdots & \vdots \\ I \left[\frac{^{36}\text{Ar}^b(ca, t_n)}{^{37}\text{Ar}^b(ca, t_n)} \right] & I \left[\frac{^{39}\text{Ar}^b(ca, t_n)}{^{37}\text{Ar}^b(ca, t_n)} \right] \end{bmatrix} \quad (95)$$

resulting in a vector of logratio intercepts $X(ca)$ and covariance matrix $\Sigma_{X(ca)}$. For the detector calibration, we replace Eq. (29) with:

$$X^*(ca) = [X(ca) \ Z(d[37]) \ Z(d[39]) \ Z(d[40])] \quad (96)$$

with covariance matrix $\Sigma_{X^*(ca)}$:

$$\Sigma_{X^*(ca)}^* = \begin{bmatrix} \Sigma_{X(ca)} & 0_{2,1} & 0_{2,1} & 0_{2,1} \\ 0_{1,2} & \sigma[Z(d[37])]^2 & 0 & 0 \\ 0_{1,2} & 0 & \sigma[Z(d[39])]^2 & 0 \\ 0_{1,2} & 0 & 0 & \sigma[Z(d[40])]^2 \end{bmatrix} \quad (97)$$

where, for the sake of notational simplicity, we have assumed that only a single Ca-salt measurement was made (accommodating duplicate analyses is trivial). Note that

Eqs. (96) and (97) use $Z(d[40])$ instead of $Z(d[36])$, implying equal sensitivities of detectors $d[36]$ and $d[40]$. This assumption is valid because the sensitivity difference between said detectors is accounted for by the mass fractionation correction. Eqs. (31) and (32) remain the same but use the following Jacobian matrix:

$$J'_{C(ca)} = \begin{bmatrix} 1 & 0 & 1 & 0 & -1 \\ 0 & 1 & 1 & -1 & 0 \end{bmatrix} \quad (98)$$

We thus obtain a two-element vector of sensitivity-corrected logratio intercepts $C(ca)$ and its covariance matrix $\Sigma_{C(ca)}$. For the mass fractionation correction, we first append the air shot data to the calibration-corrected logratio intercepts:

$$C^*(ca) = \left[C(ca) \ A(37) \ I \left[\frac{^{40}\text{Ar}}{^{36}\text{Ar}} \right]_a \right] \quad (99)$$

with $[4 \times 4]$ covariance matrix $\Sigma_{C^*(ca)}^*$:

$$\Sigma_{C^*(ca)}^* = \begin{bmatrix} \Sigma_{C(ca)} & 0_{2,1} & 0_{2,1} \\ 0_{1,2} & \sigma[A(37)]^2 & 0 \\ 0_{1,2} & 0 & 0 \end{bmatrix} \quad (100)$$

Recasting in matrix form, the fractionation-corrected Ca-salt measurements and their covariances are given by:

$$F(ca) = C^*(ca) J_{F(ca)} \quad (101)$$

and

$$\Sigma_{F(ca)} = J'_{F(ca)} \Sigma_{C^*(ca)}^* J_{F(ca)} \quad (102)$$

respectively, where $J_{F(ca)}$ is the Jacobian matrix of the mass fractionation calibration and $J'_{F(ca)}$ its transpose:

$$J'_{F(ca)} = \begin{bmatrix} 1 & 0 & -0.240 & -0.240 \\ 0 & 1 & 0.487 & 0.487 \end{bmatrix} \quad (103)$$

For 'peak hopping' data, Eq. (95) may be replaced with three vectors containing the logs of the time-resolved ^{36}Ar , ^{37}Ar and ^{39}Ar signals, which can be processed as in Section 4 to calculate the logratio intercepts. Since detector calibration does not apply to single collector instruments, Eqs. (96)–(103) can be safely skipped. Next, we apply the decay correction which, as explained in Section 7, affects both ^{37}Ar and ^{39}Ar . At this point the data reduction of the Ca and K-interference monitors is merged with that of the samples and fluence monitors. This is achieved by collating their respective decay corrections:

$$r(i)' = \begin{bmatrix} r(\lambda_i, \tau[u_1]) \\ r(\lambda_i, \tau[s_1]) \\ r(\lambda_i, \tau[u_2]) \\ r(\lambda_i, \tau[s_2]) \\ r(\lambda_i, \tau[s_3]) \\ r(\lambda_i, \tau[ca]) \\ r(\lambda_i, \tau[k]) \end{bmatrix} \quad (104)$$

the covariance matrices of which are given by Eq. (45) with

$$J'_{r(i)} = \begin{bmatrix} \frac{\partial r(\lambda_i, \tau | u_1)}{\partial \lambda_i} \\ \frac{\partial r(\lambda_i, \tau | s_1)}{\partial \lambda_i} \\ \frac{\partial r(\lambda_i, \tau | u_2)}{\partial \lambda_i} \\ \frac{\partial r(\lambda_i, \tau | s_2)}{\partial \lambda_i} \\ \frac{\partial r(\lambda_i, \tau | s_3)}{\partial \lambda_i} \\ \frac{\partial r(\lambda_i, \tau | ca)}{\partial \lambda_i} \\ \frac{\partial r(\lambda_i, \tau | k)}{\partial \lambda_i} \end{bmatrix} \quad (105)$$

To apply these decay corrections, we append them to the fractionation-corrected logratios:

$$F^* = [F \ F(ca) \ F(k) \ r(37) \ r(39)] \quad (106)$$

with $[37 \times 37]$ covariance matrix

$$\Sigma_F^* = \begin{bmatrix} \Sigma_F & 0_{20,2} & 0_{20,1} & 0_{20,7} & 0_{20,7} \\ 0_{2,20} & \Sigma_{F(ca)} & 0_{2,1} & 0_{2,7} & 0_{2,7} \\ 0_{1,20} & 0_{1,2} & \Sigma_{F(k)} & 0_{1,7} & 0_{1,7} \\ 0_{7,20} & 0_{7,2} & 0_{7,1} & \Sigma_{r(37)} & 0_{7,7} \\ 0_{7,20} & 0_{7,2} & 0_{7,1} & 0_{7,7} & \Sigma_{r(39)} \end{bmatrix} \quad (107)$$

These values are then simply plugged into Eqs. (50) and (51):

$$I = F^* J_D \quad (108)$$

$$\Sigma_I = J_D^* \Sigma_F^* J_D \quad (109)$$

where J_D is the $[37 \times 23]$ Jacobian matrix and J_D^* its transpose:

$$J_D^* = [1_{23,23} \ J_{D(37)}^* \ J_{D(39)}^*] \quad (110)$$

with

$$J_{D(37)}^* = \begin{bmatrix} J_{D(37)}^{**} & 0_{4,1} & 0_{4,1} & 0_{4,1} & 0_{4,1} & 0_{4,1} & 0_{4,1} & 0_{4,1} \\ 0_{4,1} & J_{D(37)}^{**} & 0_{4,1} & 0_{4,1} & 0_{4,1} & 0_{4,1} & 0_{4,1} & 0_{4,1} \\ 0_{4,1} & 0_{4,1} & J_{D(37)}^{**} & 0_{4,1} & 0_{4,1} & 0_{4,1} & 0_{4,1} & 0_{4,1} \\ 0_{4,1} & 0_{4,1} & 0_{4,1} & J_{D(37)}^{**} & 0_{4,1} & 0_{4,1} & 0_{4,1} & 0_{4,1} \\ 0_{4,1} & 0_{4,1} & 0_{4,1} & 0_{4,1} & J_{D(37)}^{**} & 0_{4,1} & 0_{4,1} & 0_{4,1} \\ 0 & 0 & 0 & 0 & 0 & -1 & 0 & 0 \\ 0 & 0 & 0 & 0 & 0 & -1 & 0 & 0 \\ 0 & 0 & 0 & 0 & 0 & 0 & 0 & 0 \end{bmatrix} \quad (111)$$

and

$$J_{D(39)}^* = \begin{bmatrix} J_{D(39)}^{**} & 0_{4,1} & 0_{4,1} & 0_{4,1} & 0_{4,1} & 0_{4,1} & 0_{4,1} & 0_{4,1} \\ 0_{4,1} & J_{D(39)}^{**} & 0_{4,1} & 0_{4,1} & 0_{4,1} & 0_{4,1} & 0_{4,1} & 0_{4,1} \\ 0_{4,1} & 0_{4,1} & J_{D(39)}^{**} & 0_{4,1} & 0_{4,1} & 0_{4,1} & 0_{4,1} & 0_{4,1} \\ 0_{4,1} & 0_{4,1} & 0_{4,1} & J_{D(39)}^{**} & 0_{4,1} & 0_{4,1} & 0_{4,1} & 0_{4,1} \\ 0_{4,1} & 0_{4,1} & 0_{4,1} & 0_{4,1} & J_{D(39)}^{**} & 0_{4,1} & 0_{4,1} & 0_{4,1} \\ 0 & 0 & 0 & 0 & 0 & 0 & 0 & 0 \\ 0 & 0 & 0 & 0 & 0 & 0 & 1 & 0 \\ 0 & 0 & 0 & 0 & 0 & 0 & 0 & 1 \end{bmatrix} \quad (112)$$

with $J_{D(37)}^{**}$ and $J_{D(39)}^{**}$ as in Eq. (54). This completes the Ca-interference correction. The K-interference on ^{40}Ar and (as discussed in Appendix B) ^{38}Ar , can be corrected

in a very similar manner by monitoring $^{40}\text{Ar}/^{39}\text{Ar}$ and $^{38}\text{Ar}/^{39}\text{Ar}$ in K-glass.

APPENDIX B. CL-INTERFERENCE CORRECTION ACCOUNTING FOR ALL SOURCES OF ^{38}Ar

As mentioned at the end of Section 9, the Cl-interference correction on ^{36}Ar implemented in Eq. (5) does not account for the presence of atmospheric ^{38}Ar or the production of ^{38}Ar from K. Doing so is straightforward but requires a reformulation of Eq. (5):

$$R = \frac{1 - a + b + c - g - h + i}{d - e - j + k} - f \quad (113)$$

with $a-f$ as defined in Eq. (5)

$$g = \left[\frac{^{38}\text{Ar}}{^{36}\text{Ar}} \right]_a \left[\frac{^{36}\text{Ar}}{^{38}\text{Ar}} \right]_{cl} \quad (114)$$

$$h = \left[\frac{^{40}\text{Ar}}{^{36}\text{Ar}} \right]_a \left[\frac{^{36}\text{Ar}}{^{38}\text{Ar}} \right]_{cl} \left[\frac{^{38}\text{Ar}}{^{39}\text{Ar}} \right]_k \left[\frac{^{39}\text{Ar}}{^{40}\text{Ar}} \right]_m \quad (115)$$

$$i = \left[\frac{^{40}\text{Ar}}{^{36}\text{Ar}} \right]_a \left[\frac{^{36}\text{Ar}}{^{38}\text{Ar}} \right]_{cl} \left[\frac{^{38}\text{Ar}}{^{39}\text{Ar}} \right]_k \left[\frac{^{39}\text{Ar}}{^{37}\text{Ar}} \right]_{ca} \left[\frac{^{37}\text{Ar}}{^{40}\text{Ar}} \right]_m \quad (116)$$

$$j = \left[\frac{^{38}\text{Ar}}{^{36}\text{Ar}} \right]_a \left[\frac{^{36}\text{Ar}}{^{38}\text{Ar}} \right]_{cl} \left[\frac{^{39}\text{Ar}}{^{40}\text{Ar}} \right]_m \quad (117)$$

$$k = \left[\frac{^{38}\text{Ar}}{^{36}\text{Ar}} \right]_a \left[\frac{^{36}\text{Ar}}{^{38}\text{Ar}} \right]_{cl} \left[\frac{^{39}\text{Ar}}{^{37}\text{Ar}} \right]_{ca} \left[\frac{^{37}\text{Ar}}{^{40}\text{Ar}} \right]_m \quad (118)$$

This formulation requires adjustment of Sections 10 and 11 and the addition of the $\left[\frac{^{38}\text{Ar}}{^{39}\text{Ar}} \right]_k$ to Section 8, which is omitted here for brevity.

APPENDIX C. A BRIEF INTRODUCTION TO AR-AR_REDUX

In its present form, Ar-Ar_Redux exists as a package in a statistical programming environment called R. After installing R from <http://r-project.org>, Ar-Ar_Redux can be installed by typing

```
install.packages('ArArRedux')
```

Once installed, the package can be loaded by typing `library(ArArRedux)`

The first step in the data reduction procedure is to load the time resolved mass spectrometer signals and turn them into a vector of logratio intercepts with associated covariance matrix. The `read` function groups the calculations listed in Sections 3–5:

```
X <- read(xfile="Samples.csv",
  masses=c("Ar37","Ar38","Ar39","Ar40","Ar36"),
  blabel="BLANK#", Jpos=c(3,15),
  kfile="K-glass.csv",
  cafile="Ca-salt.csv",
  dfile="Calibration.csv",
  dlabels=c("H1","AX","L1","L2")
)
```

where `xfile` is the name of a file containing the time resolved mass spectrometer data of all the samples, fluence monitors and blanks; `masses` is a vector specifying the

order in which the argon isotopes are listed within `xfile`; `blabel` is the prefix of the blanks listed in `xfile`; `Jpos` is a vector with the positions of the fluence monitors within the irradiation stack; `kfile` is the name of a file containing the time resolved mass spectrometer signals of co-irradiated K-bearing monitor glass, formatted in the same way as `xfile`; `cafile` contains the same information for the co-irradiated Ca-bearing salts; `dfile` contains the detector intercalibration data and `dlabels` is a list specifying the order in which the detectors are listed within `dfile`. Next, we form a list of two fractionation corrections, one for each denominator isotope used in Eq. (5) (i.e. ^{37}Ar , ^{39}Ar and ^{40}Ar):

```
fract <- list (
  fractionation("L2.csv",detector="L2",PH=TRUE),
  fractionation("AX.csv",detector="AX",PH=TRUE),
  fractionation("H1.csv",detector="H1",PH=FALSE)
)
```

where the `fractionation` function performs the calculations outlined in Section 6 and Appendix A; `detector` specifies the name of the detector of interest; and `PH` is a boolean flag indicating whether the data are collected in multicollector or ‘peak hopping’ mode. The last file that needs to be loaded contains the neutron irradiation schedule:

```
irr <- loadirradiations("irradiations.csv")
```

The `process` function carries out the fractionation, decay and interference corrections (Sections 6–9), interpolates the *J*-factors and calculates the ages (Sections 11 and 12):

```
ages <- process(X,irr,fract)
```

The following three lines are used to tabulate the results, view the covariance structure as a coloured correlation matrix, and calculate the weighted mean age of a subset (in this example samples S1–5) of the data, respectively:

```
summary(ages)
corrplot(ages)
weightedmean(ages,c("S1","S2","S3","S4","S5"))
```

Ar–Ar_Redux is very flexible. For example, all but the first four arguments to the `read` function are optional. If, for instance, no co-irradiated K-glass or Ca-salt were analysed, then it is possible to specify the interference corrections explicitly. A comprehensive overview of all the options falls outside the scope of this short Appendix. A more extensive tutorial is provided on <http://redux.london-geochron.com>. Contextual help within the R environment can be obtained from Ar–Ar_Redux’s built-in documentation. For example, to learn more about the `read` function, it suffices to type `?read` at the command prompt.

REFERENCES

Aitchison J. (1986) *The Statistical Analysis of Compositional Data*. Chapman and Hall, London.

- Berger G. W. and York D. (1970) Precision of the $^{40}\text{Ar}/^{39}\text{Ar}$ dating technique. *Earth Planet. Sci. Lett.* **9**, 39–44.
- Bowring J., McLean N. and Bowring S. (2011) Engineering cyber infrastructure for U–Pb geochronology: Tripoli and U–Pb_Redux. *Geochem. Geophys. Geosyst.* **12**.
- Foland K., Fleming T., Heimann A. and Elliot D. (1993) Potassium-argon dating of fine-grained basalts with massive Ar loss: application of the $^{40}\text{Ar}/^{39}\text{Ar}$ technique to plagioclase and glass from the Kirkpatrick Basalt, Antarctica. *Chem. Geol.* **107**, 173–190.
- Koppers A. A. (2002) ArArCALC – software for $^{40}\text{Ar}/^{39}\text{Ar}$ age calculations. *Comput. Geosci.* **28**, 605–619.
- Kuiper K. F., Deino A., Hilgen F. J., Krijgsman W., Renne P. R. and Wijbrans J. R. (2008) Synchronizing rock clocks of earth history. *Science* **320**, 500–504.
- Lee J. Y., Marti K., Severinghaus J. P., Kawamura K., Yoo H. S., Lee J. B. and Kim J. S. (2006) A redetermination of the isotopic abundances of atmospheric Ar. *Geochim. Cosmochim. Acta* **70**, 4507–4512.
- McDougall I. and Harrison T. M. (1999) *Geochronology and Thermochronology by the $^{40}\text{Ar}/^{39}\text{Ar}$ Method*. Oxford University Press, New York.
- McLean N., Bowring J. and Bowring S. (2011) An algorithm for U–Pb isotope dilution data reduction and uncertainty propagation. *Geochem. Geophys. Geosyst.* **12**.
- Min K., Mundil R., Renne P. R. and Ludwig K. R. (2000) A test for systematic errors in $^{40}\text{Ar}/^{39}\text{Ar}$ geochronology through comparison with U/Pb analysis of a 1.1-Ga rhyolite. *Geochim. Cosmochim. Acta* **64**, 73–98.
- Nelder J. A. and Wedderburn R. W. M. (1972) Generalized linear models. *J. R. Stat. Soc. Ser. A–G* **135**(3), 370–384.
- Renne P. R. and Norman E. B. (2001) Determination of the half-life of ^{37}Ar by mass spectrometry. *Phys. Rev. C* **63**, 047302.
- Renne P. R., Swisher C. C., Deino A. L., Karner D. B., Owens T. L. and DePaolo D. J. (1998) Intercalibration of standards, absolute ages and uncertainties in $^{40}\text{Ar}/^{39}\text{Ar}$ dating. *Chem. Geol.* **145**, 117–152.
- Renne P. R., Sharp Z. D. and Heizler M. T. (2008) Cl-derived argon isotope production in the CLICIT facility of OSTR reactor and the effects of the Cl-correction in $^{40}\text{Ar}/^{39}\text{Ar}$ geochronology. *Chem. Geol.* **255**, 463–466.
- Scaillet S. (2000) Numerical error analysis in $^{40}\text{Ar}/^{39}\text{Ar}$ dating. *Chem. Geol.* **162**, 269–298.
- Stoener R., Schaeffer O. and Katcoff S. (1965) Half-lives of argon-37, argon-39, and argon-42. *Science* **148**, 1325–1328.
- Vermeesch P. (2010) HelioPlot, and the treatment of overdispersed (U–Th–Sm)/He data. *Chem. Geol.* **271**, 108–111.
- Wijbrans J. R. and McDougall I. (1986) $^{40}\text{Ar}/^{39}\text{Ar}$ dating of white micas from an Alpine high-pressure metamorphic belt on Naxos (Greece): the resetting of the argon isotopic system. *Contrib. Mineral. Petrol.* **93**, 187–194.
- Wood S. N. (2015) *Core Statistics*, 1st ed. Cambridge University Press, ISBN 9781107415041, p. 258.
- York D. (1968) Least squares fitting of a straight line with correlated errors. *Earth Planet. Sci. Lett.* **5**, 320–324.
- Young E. D., Galy A. and Nagahara H. (2002) Kinetic and equilibrium mass-dependent isotope fractionation laws in nature and their geochemical and cosmochemical significance. *Geochim. Cosmochim. Acta* **66**, 1095–1104.

Associate editor: Chris M. Hall